

7
73/79
248 XT 15

SAND79-0745
Unlimited Release

MASTER

Preliminary Results Report Conasauga Near-Surface Heater Experiment

James L. Krumhansl



Sandia Laboratories

SF 2900 O17-731

DISTRIBUTION OF THIS DOCUMENT IS UNLIMITED

PRELIMINARY RESULTS REPORT
CONASAUGA NEAR-SURFACE HEATER EXPERIMENT

James L. Krumhansl
Geological Projects Division 4537
Sandia Laboratories, Albuquerque, NM 87185

ABSTRACT

From November 1977 to August 1978, two near-surface heater experiments were operated by Sandia Laboratories at Oak Ridge, Tennessee. The experiments were sited in two somewhat different stratigraphic sequences within the Conasauga formation which consist predominantly of shale. Specific phenomena investigated were the thermal and mechanical responses of the formation to an applied heat load, as well as the mineralogical changes induced by heating. The program's objective was to provide a minimal integrated field and laboratory study that would supply a data base which could be used in planning more expensive and complex vault-type experiments in other localities. The experiments were operated with heater power levels of between 6 and 8 kW for heater mid-plane temperatures of 385°C. The temperature fields within the shale were measured and analysis is in progress. Steady state conditions were achieved within 90 days. Conduction appears to be the principal mechanism of heat transport through the formation. Limited mechanical response measurements consisting of vertical displacement and stress data indicate general agreement with predictions. Posttest data, collection of which await experiment shutdown and cooling of the formation, include the mineralogy of posttest cores, posttest transmissivity measurements and corrosion data on metallurgical samples.

NOTES

This report was prepared as an account of work sponsored by the United States Government. Neither the United States nor the United States Department of Energy, nor any of their employees, nor any of their contractors, subcontractors, or their employees, makes any warranty, express or implied, or assumes any legal liability or responsibility for the accuracy, completeness, or usefulness of any information, apparatus, product or process disclosed, or represents that its use would not infringe upon privately owned rights.

A. KNOWLEDGMENT

The author gratefully acknowledges the many individuals who contributed to the success of the project. Special recognition is due to the following Sandia Laboratory personnel for their respective efforts.

E. A. Ames	Transducer Design and Installation (Thermocouples, Stress Gauges Extensometers, Pressure Gauges)
A. J. Anaya	Thermal Conductivity and Thermal Expansion Measurements on Core Samples
A. C. Arthur	Mechanical Design
J. W. Braithwaite	Metallurgical Experiment
F. J. Conrad	Gas Analysis
R. L. Courtney	Thermal Expansion, Heat Capacity, SEM, DTA, and TGA Laboratory Measurements on Consauga Core Samples
C. O. Duimstra	Instrumentation Project Engineer
R. D. Klett	Transmissivity Modeling
J. T. Lindman	Instrument Van Operation
D. F. McVey	Thermal Modeling
C. D. Northam	Transmissivity
W. D. Sundberg	Thermal Modeling
J. R. Tillerson	Mechanical Modeling
W. Wawersik	Rock Mechanics Laboratory Measurements
W. C. Wilson	Construction Project Engineer and Transmissivity Measurements
S. F. Yager	Wattmeter Design

The site support provided by Luther Lavell and Dow Odum of Oak Ridge National Laboratory Plant Engineering during construction and experiment operation contributed greatly to helping the project proceed efficiently.

CONTENTS

	<u>Page</u>
I. INTRODUCTION	11
II. SITE GEOLOGY AND HYDROLOGY	14
III. EXPERIMENT AND HEATER DESIGN	18
Thermal Measurements	18
Stress and Displacement Measurements	24
Transmissivity Measurements	22
Pressure Measurements	23
Heater Design	24
Data Acquisition System	27
Site Layout	30
IV. EXPERIMENT INSTALLATION	31
Thermocouples	31
Extensometers	31
Pressure Measurements	31
Stress Gauges	32
Heater	32
V. HEATER OPERATIONS	36
VI. PRELIMINARY RESULTS	39
Laboratory Program	39
Modeling	45
Field Experimental Data	49

CONTENTS (cont)

	<u>Page</u>
VII. SUMMARY AND CONCLUSIONS	58
Site Selection	58
Heater Design	59
Site Instrumentation	60
Instrumentation Development	62
Laboratory and Modeling Activities	63
References	64
APPENDIX A - Grout Specifications	65

TABLES

<u>Table</u>	<u>Page</u>
I Mineralogy of Conasauga Samples	15
II Data Channel Summary Conasauga Shale	29
III Specific Gravity of Conasauga Samples	42
IV Energy Input at Site One ($\times 10^{10}$ Joules)	52

ILLUSTRATIONS

<u>Figure</u>	<u>Page</u>
1 Geologic Section Showing Heater Positions. S2-1 and S1-1 are the heater holes at Sites 1 and 2, respectively. S1, S2 and OR were early exploratory holes.	15

ILLUSTRATIONS (cont)

<u>Figure</u>		<u>Page</u>
2	Lithologies Present in Heater Holes	16
3	Conasauga Core - 64 mm (2.5 in.) Diameter	16
4	152 mm (6 in.) Core From the Bottom of the Heater Hole at Site Two	17
5	Calculated Isotherms Used in Design of Field Experiment	19
6	Predicted Radial Temperatures as a Function of Heater Power and Time for $K = 0.9 \text{ W/m}^{\circ}\text{C}$ and $2.3 \text{ W/m}^{\circ}\text{C}$	20
7	Creare Gauge Housing Assembly	21
8	Extensometer Assembly	22
9	Pressure Gauge and Packer Assembly	23
10	Heater Design Schematic	24
11	Heater Element Assembly	25
12	Completed Heater Assembly	26
13	Conasauga Experiment Instrument Van	27
14	Data Acquisition System Schematic	28
15	Data Acquisition System	29
16	Overall Site Layout, Experiment 1 Layout, Experiment 2 Layout	30
17	Heater Installation Schematic	32
18	Heater Suspended on A-Frame Preparatory to Insertion	33
19	Installation of Fiberglass Insulation	34
20	Nichrome Wire String Cutter Installation	34
21	Packer Installation	35
22	Packer Close-up	35

ILLUSTRATIONS (cont)

<u>Figure</u>		<u>Page</u>
23	Capped Heater Hole Showing Topside Gauges and Packer Sealed Conduit Feedthroughs	36
24	Heater Response Upon Turn-on in the Conasauga Near-Surface Heater Experiment	37
25	Heater Response Upon Turn-on in the Conasauga Near-Surface Heater Experiment	38
26	Heat Capacity as a Function of Temperature and Rock Type	40
27	Weight Loss as a Function of Temperature and Rock Type	41
28	Thermal Conductivities of Conasauga Samples	43
29	Thermal Expansion as a Function of Temperature and Rock Type	44
30	Node Geometry Used in CINDA	46
31	Node Geometry Used in SHAFT	47
32	Comparison Between Site One and Site Two Isotherms Parallel to Strike	50
33	Site One Radial Temperature Distribution	50
34	Site Two Radial Temperature Distribution	51
35	Comparison Between Actual and Computed Power at Site One	54
36	Comparison Between Actual and Computed Isotherms At Site One	54
37	Computed Circulation and Heat Flux	55
38	Summary of Vertical Extensometer Data	56
39	Predicted Regions of Vertical Extension and Compression	57
40	Summary of Horizontal Creep Gauge Data	57

PRELIMINARY RESULTS REPORT
CONASAUGA NEAR-SURFACE HEATER EXPERIMENT

I. INTRODUCTION

The Conasauga tests, and near surface tests in general, have the common goal of contributing to the assessment of whether the rock type involved, in this case shale, can withstand the near-field thermal load from a canister of high-level nuclear waste. During such tests, it is possible to observe both the thermal and mechanical response of a formation on a scale considerably in excess of that feasible in the laboratory, and to assess whether the in situ environment can be adequately modeled using existing numerical techniques. Of particular concern during this experiment was the ability of the formation to dissipate heat in situ, a function of effective conductivity, and the question of whether or not a single heat dissipation mechanism would dominate to the extent that a relatively straightforward analysis would be possible. Secondary objectives included determination of displacements engendered by the heating process and of whether or not the texture of the formation was appreciably altered by thermal degradation of minerals, cracking due to thermal stresses, or solution and reprecipitation of new minerals by circulating ground water.

At the outset, it is to be emphasized that near-surface tests are but a step toward resolution of the complex problems associated with the disposal of nuclear waste. Beyond obvious concerns associated with extrapolating the results of such a short-term test to time periods of several hundred years, it is evident that in an actual repository the overburden and tectonic stresses would be different than that encountered during this test, and that radiation effects could significantly alter the chemistry of the system. Nevertheless, when detailed consideration is given to simulating repository conditions at depth, it becomes apparent

that a large number of competing processes may operate, and there is a dearth of data which may be used to predict the final outcome. The problem is further confounded by a virtual absence of case histories which may be used to judge laboratory tests and numerical models to predict the behavior of complex materials in natural settings. Therefore, if underground excavations are unavailable prior to embarking on expensive and time-consuming vault tests, it would be wise to implement an intermediate step for the purpose of gaining some feeling for the processes which truly are of greatest significance. The Conasauga tests were undertaken to satisfy this requirement.

Sandia Laboratories, under contract with the Office of Waste Isolation (OWI), agreed in the Fall of 1976 to do near-surface heater experiments at two adjacent sites separated by 37 meters in the Conasauga formation. The design of the proposed experiment was predicated on the following assumptions:

1. The dimensions of rock exposed to a significant thermal flux and resulting thermomechanical stress fields should be substantially greater than the scale of a laboratory experiment, which is approximately 0.03 m^3 (1 ft³).
2. The temperature of the heater should be greater than that of a potential waste canister so that temperatures and core samples more typical of a waste canister environment could be obtained readily at a location removed from the heater. Close to the heaters, both temperature measurements and core recovery were expected to be difficult.
3. The heater temperature should be less than that at which significant mineralogic decomposition occurs (assuming that it is much greater than that of a potential waste canister).

4. For practical reasons heater operating temperature would be limited to the capability of commercially available elements. Maintenance of a temperature of 600°C would be consistent with assumptions two and three as was assumed in the original proposal.
5. A minimum number of drill holes would be specified for each site commensurate with providing a) a gross picture of the heater induced thermal field, b) stress and strain levels, and c) mineralogical changes.
6. The drill hole depth assumed was 15.4 m (50 ft) for cost estimation purposes. It was further assumed that the top 9.2 m (30 ft) of all holes would be cased.
7. All instrumentation drill holes were to be in the range of 3.8 cm (1 1/2 in.) to 6.3 cm (2 1/2 in.) diameter.
8. In addition to "basic" experiments proposed, some drill holes and recording channels were included for instrument development. Their purpose would be to permit latitude for evaluation of special site specific features such as thermal stress anisotropy related to bedding plane orientation.

The Sandia proposal of May 1976, which was accepted by OWI, did not account for the possible presence of water in the formation. However, holes drilled at the sites subsequently made available for this experiment, resulting from a 5-month reconnaissance conducted by George Brunton of OWI, produced water at the rate of about 15 l/hr from a 20 cm (8 in) diameter hole. As a result, some of the plans required modification and revision. Changes included:

1. A heater mid-plane temperature of only 385°C instead of the 600°C initially proposed. The requirement for heating a credibly larger than laboratory-scale rock mass was amply met without going to 600°C.

2. Instrument drill holes were cored to 10.2 cm (4 in.) diameters instead of 3.8 to 6.4 cm (1.5 to 2.5 in.) in order to obtain 6.4 cm (2 1/2 in.) diameter core for laboratory studies.

3. The heater holes were pressurized with air to exclude water.

Subsequent sections address specific experiment design considerations and results.

11. SITE GEOLOGY AND HYDROLOGY

The geologic setting of the Conasauga Near-Surface Heater Experiment site is shown schematically in Fig. 1. Although subject to considerable local variation, bedding in the vicinity of the heaters dips generally to the southeast at about thirty degrees. In addition to a general dip, the rocks at the site have been sheared in various directions, and in places have been folded or crumpled. Although the bulk of the sediments at the sites consists of shale, the section as a whole is a rather heterogeneous assemblage of intimately interlayered fine-grained rocks. Toward the base of the section, as shown at Site One, a dark gray calcareous shale is interspersed with limestone beds ranging from one to several centimeters in thickness. Moving upward, there is a unit roughly 3 m thick consisting primarily of limestone, above which (as shown at Site Two) the formation consists of thin layers of interbedded gray-green or maroon shale with lesser amounts of siltstone. Details of the stratigraphy in the heater holes at the two sites are illustrated in Fig. 2. Figure 3 illustrates the appearance of the Conasauga at the heater site when recovered in core. A sample of the large core recovered from the central heater hole in Site Two is shown in Fig. 4. As one would infer from the lithologic heterogeneity, the mineralogy and hence chemistry of these rocks is quite variable (Table I). In the shales, illite, kaolinite, and members of the

chlorite group are the principal clay minerals, while the limestone consists primarily of calcite. Quartz and feldspar predominate in the siltstones along with lesser amounts of clays, micas, and calcite. Iron pyrite is virtually absent everywhere in the section.

TABLE I
Mineralogy of Conasauga Samples

	<u>Calcite</u>	<u>Feldspar</u>	<u>Quartz</u>	<u>Kaolinite</u>	<u>Illite</u>	<u>Chlorite</u>
Limestone	Major	Minor	Minor	-	-	-
Vein Calcite	Major	Minor	Minor	-	-	-
Gray-Green Siltstone	Minor	Major	Major	Minor	Trace	Minor
Gray-Green Shale	Minor	Major	Major	Minor	Major	Minor
Maroon Shale	-	Minor	Minor	Minor	Major	Trace
Dark Gray Shale	Minor	Minor	Minor	Minor	Major	Minor

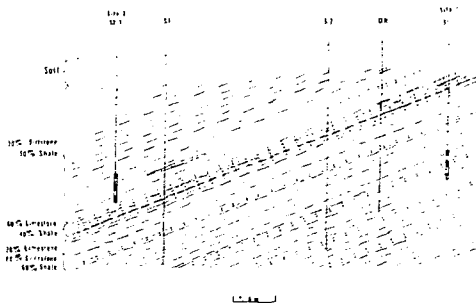


Fig. 1. Geologic Section Showing Heater Positions. S2-1 and S1-1 are the heater holes at Sites 1 and 2, respectively. S1, S2 and OR were early exploratory holes.

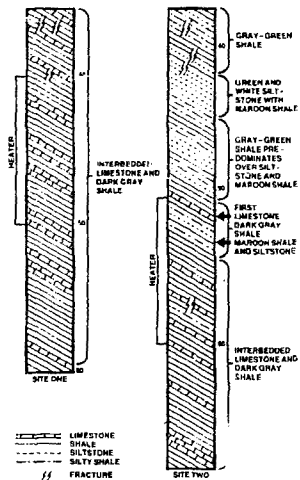


Fig. 2. Lithologies Present in Heater Holes

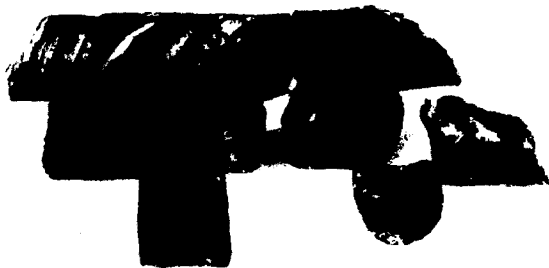


Fig. 3. Conasauga Core - 64 mm (2.5 in.) Diameter



Fig. 4. 152 mm (6 in.) Core From the Bottom of the Heater Hole at Site Two

The hydrologic setting of the experiment is largely a function of the climate and fracture network within the formation. Rainfall in the area is sufficient to maintain the water table at a relatively shallow depth, usually three to five meters below the surface. Following a heavy rain, there is a tendency for the water table to follow the topography and for water levels near Site One to be higher than at Site Two. Within a few days, however, this disappears and the three meters difference in elevation between the sites is no longer reflected by the water table. In situ permeabilities of the shale are governed predominantly by the fractures which are highly variable in distribution; consequently, there are irregular domains of greater or lesser permeability distributed throughout the area of the heater tests. At Site One, for example, a well 23 meters away along strike bubbles readily when 0.14 MPa (20 psig) air pressure is applied to the central heater hole, but it proved virtually impossible to make transmissivity measurements between the central heater hole and a hole only 3.3 meters up dip. Downhole television viewing of the two heater holes reflects the same heterogeneity of joint fracture distribution. Over vertical intervals of roughly a meter, the rock may appear devoid of open joints. One may then encounter intervals of equal

width showing irregular or folded bedding, fracturing, and obvious water recharge. In spite of these complexities, it appears that averaged permeabilities in the range of 0.001 to 0.1 darcys would account for the recharge rates observed in wells over the area of the heater site. Of specific concern are the recharge rates in the two heater holes. Immediately following completion of these wells they filled at rates of 16 and 13 l/hr at Sites One and Two, respectively.

III. EXPERIMENT AND HEATER DESIGN

Thermal Measurements

As indicated in Section I, a significant goal of the experiment was to measure the thermomechanical response of the formation, with particular emphasis on the thermal field measurements. Since the lithology along strike should be similar at all locations at a given depth, the primary instrumentation was arrayed along strike. Additional instrumentation was placed in drill holes on a line normal to strike to identify significant temperature field anisotropy.

Expected temperature fields were calculated during the course of designing the instrumentation array in order to help optimize transducer placement. Published thermal conductivities for the Conasauga shale were in the range of 0.9-2.3 W/m°C.¹ The specific heat and density values were in the vicinity of 10^3 J/°C-Kg and 2.3×10^3 Kg/m³, respectively. Figure 5 is an isotherm schematic showing a predicted temperature distribution. In preparing this figure thermal conductivity, specific heat, and density were assumed to be 0.9 W/m°C, 10^3 J/°C-Kg, and 2.3×10^3 Kg/m³, respectively. The heater is a 3 m long, 0.3 m diameter cylinder. Operated at 3.8 kW, with a surface temperature nominally 600°C above ambient, such a heater should produce the thermal field shown in Fig. 5 in a period of 400 days. Figure 6 compares the temperature profiles as a function of heating time assuming 0.9 W/m°C and 2.3 W/m°C thermal conductivities.

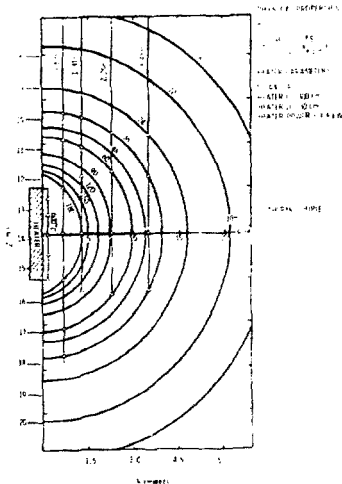


Fig. 5. Calculated Isotherms Used in Design of Field Experiment

Figure 5 also indicates approximate thermal measurement locations. One can assume that the schematic represents a vertical plane through the heater, with the orientation chosen along some significant direction at a specific site. The most important measurements are those made radially outward at the heater center-plane. However, sufficient thermocouples were installed to permit more complete determination of isotherm locations including positions below the heater. The radial coordinates for thermocouple drill holes were chosen on the basis that the measurements are desired as close together as possible where the temperature gradients are steepest. Thus, near the heater, drill holes are spaced at 0.5 to 0.6 m radial intervals. Drilling considerations make it impractical to have the holes any closer together. The drill holes at 2.25 and 3.45 m provide a reasonable coverage of the thermal field. Two thermocouples are at a 10 m radius to provide background temperature measurements.

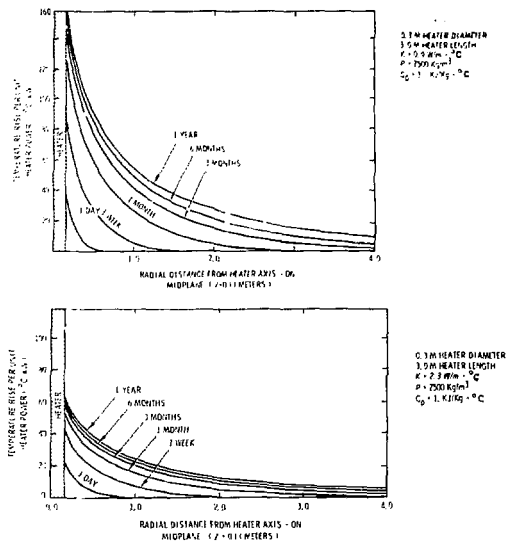


Fig. 6. Predicted Radial Temperatures as a Function of Heater Power and Time for $K = 0.9 \text{ W/m}^\circ\text{C}$ and $2.3 \text{ W/m}^\circ\text{C}$

Stress and Displacement Measurements

Minimal displacement and stress measurements were called for in the basic experiment plan. The purpose of these measurements was not to determine strain and stress fields for a complete comparison with stress models, but merely to measure the general level of stress and displacement and to attempt to correlate the two with other changes in the formation. The quoted thermal expansion value¹ of $9 \times 10^{-6} \text{ }^\circ\text{C}^{-1}$ is large enough that significant displacements should occur at the 100°C isotherm location of Fig. 5. Three drill holes per site were used for those measurements. Each contained a combination of vertical displacement extensometers and Creare stress gauges.

The Creare stress gauge is a vibrating wire gauge activated by a solenoid. Stress is determined by monitoring the frequency of the vibrating wire. For application in soft rocks such as the Conasauga, *emplacement of the gauge without some packaging modification presents several difficulties.* First, reliable emplacement of the gauge is difficult. Second, the emplacement stress may be sufficient to deform or fracture the rock. Third, the stress remaining after emplacement may be sufficient to cause subsequent plastic deformation in the rock.

To circumvent some of these difficulties, the Creare gauges in the Conasauga experiments were "set" into 1.5 mm thick aluminum tubing and potted prior to installation (Fig. 7). While installing, this assembly was fixed in place using an expandable grout. This increased the initial stress on the potted gauge by about 0.4) MPa (60 psig). Since the mode of installation differs significantly from the standard procedure, this measurement is considered to be developmental and not quantitative in nature.

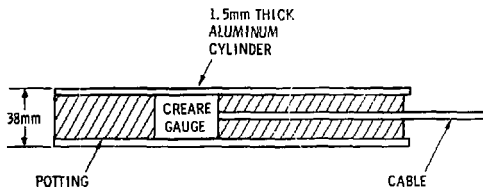


Fig. 7. Creare Gauge Housing Assembly

The displacement gauges selected were vertical extensometers. Four invar rods were anchored at different heights in each of the extensometer drill holes and extended to the bottom of the casing, where they were connected to 303 stainless steel rods that joined a potentiometer at the top of the casing. Figure 8 is a photograph of an extensometer assembly showing only one of the four rods used.

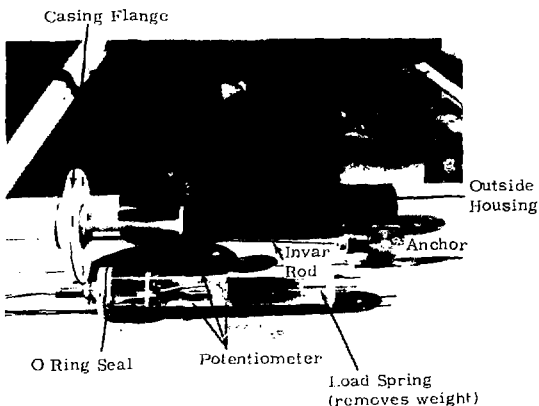


Fig. 8. Extensometer Assembly

Transmissivity measurements

To assess the fluid transport characteristics of the formation, radioactive krypton-85 tracers were injected into pressurized source wells. The time required for the pressurized air to carry the tracer to the unpressurized exit well was determined by placing an array of four Geiger-Muller probes at various depths below the casing of the exit hole. Prior to the test, ground water was removed from the major fractures and porous zones in the formation by applying air pressure of about 0.15 MPa to the formation overnight and then bleeding the formation back to atmospheric pressure in the morning. (Following this treatment it was found that the holes failed to recharge for a period of several hours.) After groundwater was removed by the above procedure, all holes, except the source and exit ones being tested, were capped and a steady state air flow was established between the two. The krypton was introduced as a pulse from a solenoid controlled gas bottle located just below the casing

in the source hole. During the test, input pressure and flow (as well as the exit flow) were monitored continuously in order to insure that steady state conditions were maintained. By noting which of the Geiger-Muller tubes responded first, it was possible to infer the location of a permeable zone; and by measuring the input and exit flow rates as well as the travel time, a semiquantitative estimate of the formation permeability between the holes was obtained.

Pressure Measurements

Gas tight packers were installed at the bottoms of the casings in the heater hole and in the three posttest transmissivity holes at each site. Holes containing extensometers were without packers, but were capped with air-tight flanges at the surface. Pressure transducers (Gulton Industries, Type GS-631) having a 0 to 0.69 MPa (0-100 psig) range were installed below the packer in those holes having packers and below the well cap in the extensometer holes. Figure 9 is a photograph of a test hole pressure gauge and packer assembly.

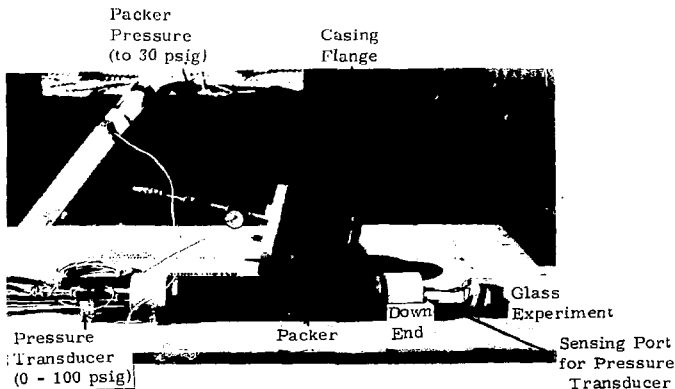


Fig. 9. Pressure Gauge and Packer Assembly

Heater Design

Figure 10 is a schematic of the heater showing the relative positions of the heated region, an insulated buffer region through which an unheated part of the heater element passes, and an air-cooled terminal region. The body of the heater consists of a sealed cylinder of 304 stainless steel. Within the heater are two complete sets of three chromalux tubular hairpin heating elements that are wired in two separate delta circuits. Rated capacity for each element is 6 kW, resulting in a maximum heater output of about 36 kW. Figure 11 is a photograph of the heater element assembly. Normal operation involved use of only one three-element set, the other remaining as backup in the event of failure of the first set. During most of the test period, the external surface of the heater at the midplane was maintained at 385°C, corresponding to a surface temperature on the chromalux elements of about 450°C and to total power consumption of between 6 and 8 kW.

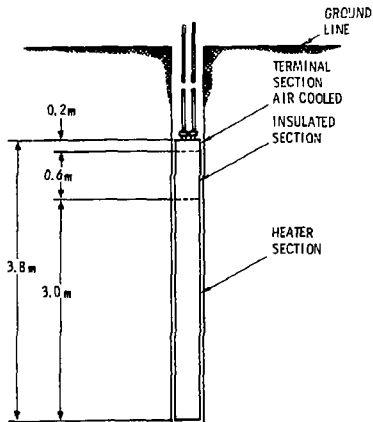


Fig. 10. Heater Design Schematic

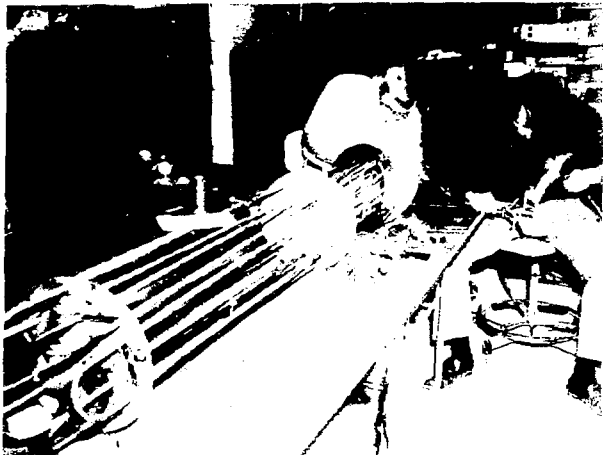


Fig. 11. Heater Element Assembly

Figure 12 is a photograph of the completed heater. Two conduits extended from the heater to the surface. The first carries the heater leads to the terminal region of the heater, and is the inlet used for cooling air for the terminals. The second conduit carries internal heater diagnostic thermocouples to the surface, as well as serving as the exhaust for the cooling air.

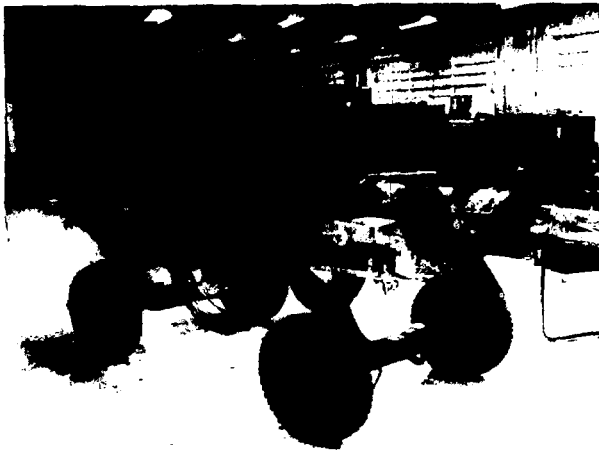


Fig. 12. Completed Heater Assembly

On the exterior surface of the heater, thermocouples were affixed on a vertical line at distances of 0.09 m (0.3 ft), 0.77 m (2.5 ft), 1.5 m (5 ft), 2.3 m (7.5 ft), 3.3 m (10.7 ft), and 3.8 m (12.3 ft) from the bottom of the heater. The exterior thermocouple at 1.5 m (5 ft) was used to control heater output during the experiment. Internal thermocouples were installed both in the terminal section (to determine whether overheating was occurring in this critical region), and on the heater elements themselves to aid in monitoring the condition of the elements during the course of the test. The air cooling was provided by a Dayton 12968 fume exhauster, operating in the suction mode. This exhauster was rated at 200 cfm at 5-inch static pressure. The measured flow rate on site was about 50 cfm.

Data Acquisition System

To the right of the instrumentation van (Fig. 13) is the emergency backup motor generator. The "demand start" unit begins the generator within 10 seconds of power interruption.

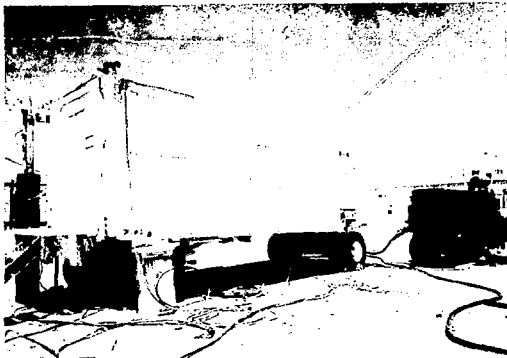


Fig. 13. Conasauga Experiment Instrument Van

Figure 14 is a schematic of the Data Acquisition System installed in the van. The system centers about the John Fluke data logger which converts the millivolt output from the thermocouples to °C and records thermocouple (TC) channels both on paper tape and the Techtran Cassette tape recorder. Vertical displacement and pressure data require signal conditioning prior to entering the data logger. The Irad-Creare gauge, clock, and wattmeter data must be converted to analog format before entering the data logger. A microprocessor linked to the John Fluke data logger controls data output to a DTC printout terminal.

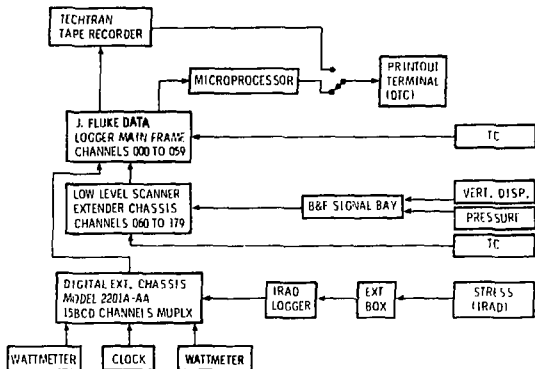


Fig. 14. Data Acquisition System Schematic

The terminal has 14 sheets of computer printout paper taped into a loop. Each sheet has from 11 to 14 channel headings. The microprocessor controls the initial printout of the data channel headings and subsequent data printout and printout paper advance so that data for each channel appears sequentially in time.

The two temperature control units are mounted on the wall to the left of the Data Acquisition System installation (see Fig. 15). The instrument rack, left bay, top to bottom, contains the Techtran recorder, Irad-Creare data logger, John Fluke data logger, wattmeter, and J. Fluke extender chassis. The right bay of the rack contains primarily signal conditioning equipment. The DTC printout terminal is in the foreground.

Table II is a summary of Data Channels on the Conasauga experiments.

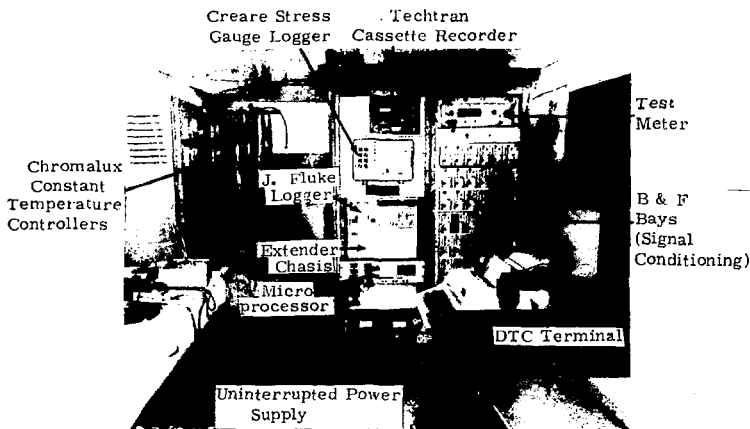


Fig. 15. Data Acquisition System

TABLE II

Data Channel Summary Conasauga Shale
Oak Ridge, Tennessee

	Experimental Array					Heater Control and Monitor	Terminal Cooling Station
	Electrode (11)	Temperature	Pressure	NO ₂	Flow		
A. Site 1 Observer Total (Depth, 50')	11 TC Chromalux Constant Type K 6 TC Chromel-Alumel Type K	11	4	3	4	1-TC Chromel/Constant Type K	2 TC Chromel-Alumel Type K
B. Site 2 Observer Total (Depth, 40')	29 TC Chromel-Conasauga Type K 2 TC Chromel-Alumel Type K	1	7	4	1	2 TC Chromel/Constant Type K	16 TC Chromel-Alumel Type K
C. Surface Environ- mental Monitoring	4 TC Chromel-Alumel Type K						
Totals	116	20	15	7	2		
Grand Total Channels	192						

Includes all TC, Chromel/Constant Type K, Chromel-Alumel Type K

Site Layout

The site of the two heater tests is located at approximately 18000 N-S and 39000 E-W on the Oak Ridge area topographic map S-16A (Maps and Survey Branch TVA, June 1974). Figure 16A is a general schematic showing the layout of Sites 1 and 2. Figures 16B and 16C are plan drawings for the individual experiments, complete with instrument summaries, for each drill hole.

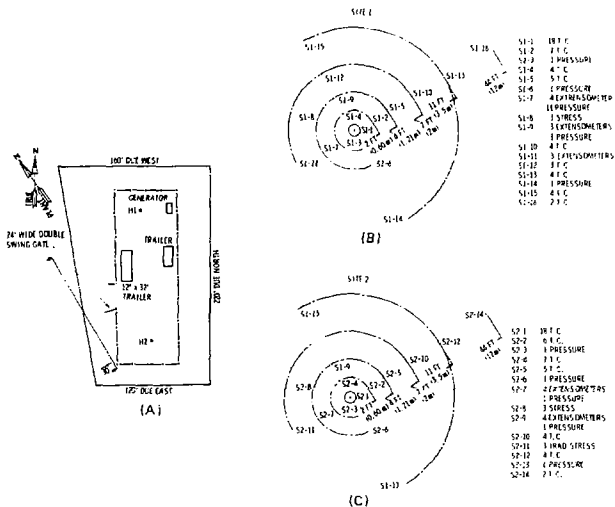


Fig. 16. (A) Overall Site Layout, (B) Experiment 1 Layout and (C) Experiment 2 Layout

PRELIMINARY RESULTS REPORT
CONASAUGA NEAR-SURFACE HEATER EXPERIMENT

James L. Krumhansl
Geological Projects Division 4537
Sandia Laboratories, Albuquerque, NM 87185

ABSTRACT

From November 1977 to August 1978, two near-surface heater experiments were operated by ~~Sandia Laboratories at Oak Ridge, Tennessee. The experiments were cited~~ in two somewhat different stratigraphic sequences within the Conasauga formation which consist predominantly of shale. Specific phenomena investigated were the thermal and mechanical responses of the formation to an applied heat load, as well as the mineralogical changes induced by heating. ~~The program's objective was to provide a minimal integrated field and laboratory study that would supply a data base which could be used in planning more expensive and complex vault-type experiments in other localities. The experiments were operated with heater power levels of between 6 and 8 kw for heater mid-plane temperatures of 385°C. The temperature fields within the shale were measured and analysis is in progress. Steady state conditions were achieved within 90 days. Conduction appears to be the principal mechanism of heat transport through the formation. Limited mechanical response measurements consisting of vertical displacement and stress data indicate general agreement with predictions. Posttest data, collection of which await experiment shutdown and cooling of the formation, include the mineralogy of posttest cores, posttest transmissivity measurements and corrosion data on metallurgical samples.~~

IV. EXPERIMENT INSTALLATION

Thermocouples

The primary thermocouples used to measure the temperature field are stainless steel sheathed chromel-constantan type E. The thermocouples were first laid out on the ground for each drill hole and tied in their desired relative positions using plastic cable ties. They were then bound to 2.5 cm diameter PVC tubing using stainless-steel hose clamps. Finally, they were lowered into drill holes with successive sections of 3 m (10 ft) lengths of PVC tubing bonded together. After all the thermocouples were installed in the drill holes, grout was pumped through the centers of the PVC tubes to fill the drill holes and cement the thermocouples in place. Grout properties are summarized in Appendix A.

Extensometers

The extensometers were anchored in position and the well caps installed. The invar rods slide through O-ring seals in the well caps. The potentiometer head assemblies (see Fig. 8) then attach to the well caps. Chromel-alumel thermocouples are attached to the anchors to permit temperature correction of the data. They also provide added temperature field data.

Pressure Measurements

The packers and the pressure gauges (see Fig. 9) beneath them were set in position near the bottom of the casings. The pressurization tube and pressure transducer cables were attached to the hole cap feed-throughs prior to bolting the caps to the hole flanges. The packers were then pressurized to about 0.21 MPa (30 psig).

Stress Gauges

Stress gauge installation was discussed in Section II under Stress and Displacement.

Heater

Figure 17 is a schematic of the heater installation. The final installation consisted of the heater with its two conduits to the surface going through: (1) a glass-wool batt, (2) a packer near the bottom of the casing, and (3) the well cap. The Dayton blower draws air into the power-lead conduit, past the terminal connectors in the heater, and out of the heater internal diagnostic thermocouple conduit.

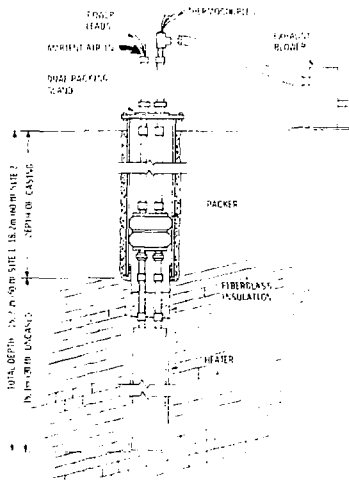


Fig. 17. Heater Installation Schematic

Figure 18 is a photograph of the heater suspended from an A-frame, preparatory to lowering it into the heater hole. No difficulty was encountered in lowering either heater. However, at Site Two a bend in the hole below the casing, and consequent bending of the conduits, resulted in a minor crack developing in one of the conduits leading back to the surface.



Fig. 18. Heater Suspended on A-Frame Preparatory to Insertion

Figure 19 shows the installation of the fiberglass insulation as it was bound tightly in place with nylon string. Upon emplacement of the heater, the nylon string is cut by passing current through a nichrome wire sandwiched between the string and asbestos cloth. Figure 20 shows the completed installation of the insulation and nichrome wire string cutter. Figure 21 shows the packer installation. Figure 22 shows the packer in more detail just prior to its being lowered into the heater hole. Finally, Fig. 23 shows the capped heater hole with the two conduits coming out of packer seals, as well as a pressure gauge and exterior heater-temperature diagnostic thermocouple lead.



Fig. 19. Installation of Fiberglass Insulation

Fig. 20. Nichrome Wire String
Cutter Installation





Figure 21. Packer Installation

Figure 22. Packer Close-up





Fig. 23. Capped Heater Hole Showing Topside Gauges and Packer Sealed Conduit Feedthroughs

V. HEATER OPERATIONS

Heater operations may be summarized by dividing the tests into two time periods. An initial 10-day period of testing was required before stable run conditions were established because of the influx of ground water into the heater holes. This was followed by an eight-month period of essentially steady state operation during which time it was possible to assess the influence of the heat source on the formation.

Most of the start-up experimentation occurred at Site One as it was the first to be activated. On the first day of operation, external air pressure was applied to exclude water from the heater hole. An experiment was then undertaken to assess whether sufficient steam pressure could be

generated in a heater hole to self-pressurize the cavity, thereby excluding additional water. This experiment was terminated after two days due to packer failure; however, during this time a pressure of 0.054 MPa (8 psig) was generated. It was decided to continue the test with the application of 0.08 MPa (12 psig) air pressure to the heater hole. This pressure was sufficient to prevent water from inundating the heater, but not to completely exclude water from the bottom few inches of the hole. Consequently, a continuous supply of steam from the bottom of the hole condensed on the conduits above the heater and dripped to the top of the heater causing erratic temperature variations on the upper part of the heater proper, as shown in Fig. 24. Based on the experience gained at Site One, the experiment at Site Two was started with sufficient air pressure, 0.19 MPa (28 psig), to completely exclude water from the heater hole. Therefore, that heater's temperature was raised in a more controlled manner than had been possible at Site One. (See Fig. 25.)

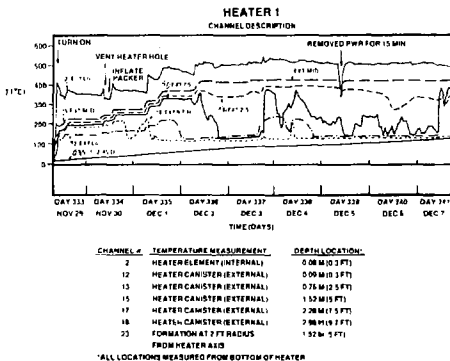


Fig. 24. Heater Response Upon Turn-on in the Conasauga Near-Surface Heater Experiment

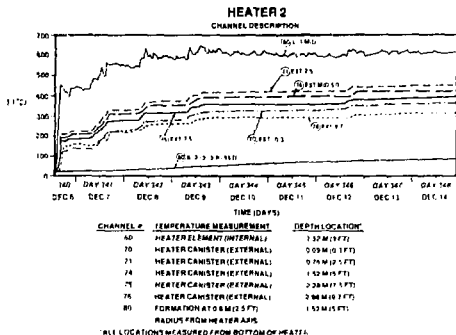


Fig. 25. Heater Response Upon Turn-on in the Conasauga Near-Surface Heater Experiment

Once a method for controlling water in the heater holes had been determined, long-term operating procedures were established. It was apparent that even at relatively high power levels, heater temperatures approaching 600°C could not be obtained. It was decided that since the system had stabilized with a heater temperature of around 385°C, and since this temperature was sufficient to heat the desired volume of rock, further perturbation should not be introduced by increasing heater power. After thirty days operation, the power input at the two sites which was required to maintain a 385°C temperature was between 6 and 8 kW; this decreased very slowly with time. Site Two consistently required about 1 kW more energy than Site One; this difference is ascribed to the heating of a greater volume of flowing air which was required to maintain a higher pressure. A second consequence of the greater air pressure at Site Two was that it resulted in a relatively dry heater hole during most of the test. In contrast to the temperature at Site One, Site Two temperatures at either end of the heater were well above 100°C during most of the test. The thermocouples at the top of the Site Two heater failed to show the erratic temperature variations caused by steam condensing at the top of the hole as observed at Site One. Finally, it should be noted that under the conditions described above both heaters functioned satisfactorily for the entire test period.

VI. PRELIMINARY RESULTS

Laboratory Program

Of particular concern in underground repository design, is the ability of the rock to dissipate heat generated by nuclear waste without incurring unacceptable changes in the thermal or mechanical properties of the formation. Consequently, the principal modeling efforts for the program have been directed toward matching field data with predictions from thermal and thermo-mechanical response codes. As input, these codes require a variety of physical parameters, hence a laboratory program was initiated to measure these variables on such core material as was available. Heat capacity, density, and thermal conductivity are required as functions of temperature for a simple conduction solution in the case of thermal codes. If fluid motion is also to be considered, additional data on porosity, permeability, water content and fluid viscosity are required. Mechanical modeling requires knowledge of thermal expansion characteristics, elastic properties of the formation, and the temperature field as a function of time. Had the formation been relatively uniform and dry, obtaining these properties might have been relatively straightforward. Unfortunately, there were a number of complications. The various rock types within the Conasauga are sufficiently different and required separate determination on each lithology, a factor aggravated by a paucity of core material of sufficient size. Mere desiccation affected many properties far more than other changes the rock might have experienced over the temperature intervals considered for this experiment. Indeed, drying or wetting of most argillaceous samples caused their complete disaggregation. Unless the extent and rate of desiccation during a laboratory determination fortuitously matches that which occurs in the field, additional interpretation is required before such data can be used in modeling. Consequently, emphasis in the laboratory program was placed on assessing the amount of variation introduced by these factors, rather than attempting to gain highly precise determinations on a few samples.

Heat Capacity

Heat capacities as a function of temperature are illustrated in Fig. 26. It should be noted that there is a reasonably wide range of values and that there is some grouping by lithology. Measurements were made using a Dupont Model 910 Thermal Analyzer, and the actual values were derived by comparison with a sapphire standard. As mentioned previously, water evolution serves as an additional complication and its impacts are included in the measurements. It is probable that this is the cause of the marked decline noted for some samples between 75° and 150°C.

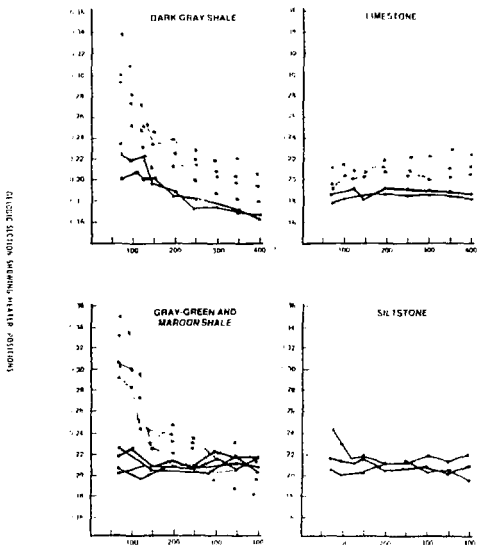


Fig. 26. Heat Capacity (cal/g-°C) as a Function of Temperature (°C) and Rock Type. (The dark lines represent air dried samples.) To convert to J/°C-Kg multiply by 4.18×10^3 .

Figure 27 summarizes thermal gravimetric analyses done on samples to assess the magnitude of the problem. For shales, we observe an immediate loss of sorbed water upon heating. At temperatures above about 450°C loss of structural water from the clay minerals begins. The decomposition of limestone (CaCO_3) beginning at about 650°C is also apparent. It would appear that shale generally loses several percent of its weight in moisture at relatively low temperatures, and that the other rock types lose less. Unfortunately, the maximum sample weight that can be handled is 0.5 g. It is probable that fractures present in larger samples would retain additional water; a larger sample would be expected to show even greater weight loss.

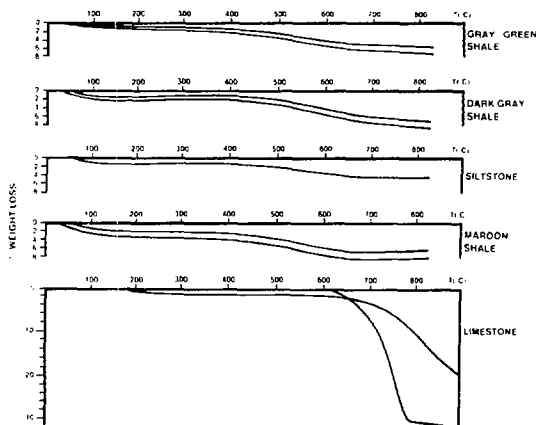


Fig. 27. Weight Loss as a Function of Temperature and Rock Type

Specific Gravity

Table III contains a summary of the specific gravities of the various rock types at the heater site. These measurements were made by first noting the weight of a sample and then measuring the water it displaced. Although there may have been some water uptake by the sample, it is unlikely that it was more than a few percent; hence the measurements are well within the accuracy needed for thermal modeling.

TABLE III

Specific Gravity of Conasauga Samples

Siltstone	2.7 ± 0.2
Dark Gray Shale	2.7 ± 0.4
Limestone	2.6 ± 0.1
Maroon and Gray Green Shale	2.7 ± 0.1

Thermal Conductivities

Temperature dependent thermal conductivities for three core samples of Conasauga Shale are shown in Fig. 28. These determinations were made on core samples 6.35 cm (2.5 in.) in diameter and roughly 7 cm long. A heater was placed at one end and a heat flux transducer at the other. The sides of the core were packed with insulation having a known thermal conductivity. Thermocouples were placed in the insulation and in a series of small drill holes along the axis of the core. From the temperature gradient at the cool end of the sample and the heat flux measured on the transducer, it was possible to directly determine thermal conductivities once a steady state had been achieved. These determinations were limited to less than 200°C, however, by the capabilities of the transducer. The higher temperature determinations were obtained by matching observed temperature profiles at the hot end of the sample with predictions based on known input wattages at the heater and the thermal properties of the insulation.

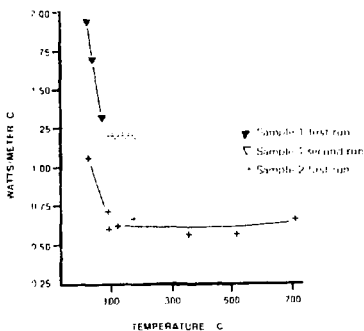


Fig. 28. Thermal Conductivities of Conasauga Samples

From Fig. 28, it is apparent that there is a precipitous decrease in thermal conductivity between room temperature and 100°C during measurements at ambient pressure. As there are no mineralogic reactions at these temperatures, it is probable that this change is caused by increased contact resistance along cracks as the sample dries. In fact, posttest sample examination, as well as examination of samples which have simply dried, reveals the presence of numerous hairline cracks. To test this hypothesis, a number of thermal comparator measurements were made at room temperature on samples which had been air dried and then rehydrated overnight in a beaker of water. Increases in conductivity in excess of thirty percent of the dry values were not uncommon with rehydration. It follows that the magnitude and position of the drop is an artifact of how the determination is made, and that under confining pressure such a drop might not be observed.

Thermal Expansion

As would be expected from their differing mineralogies, the thermal expansion of the various rock types is rather distinct (Fig. 29). Limestone and those siltstones in which quartz and feldspar predominate over clay minerals show a monotonic expansion with temperature. In

samples rich in clay, however, there is an initial thermal contraction followed by a slow expansion. Figure 29 contains two types of data regarding the behavior of argillaceous rocks. Those samples exhibiting a shallow trough were air dried prior to measurement, those that were visibly wet prior to starting the run showed several percent contraction. One sample that was merely dried at room temperature showed a two percent decrease in length during drying. One additional observation has bearing on the problem at hand. Some shale samples showed a slight thermal expansion prior to contracting. In an environment in which there was no place for water to evaporate, it is probable that this expansion would persist until the boiling point of water at which point contraction would be expected.

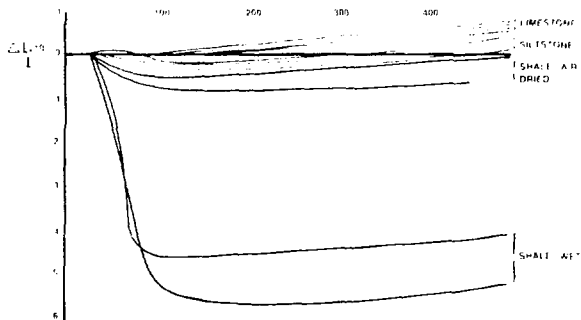


Fig. 29. Thermal Expansion as a Function of Temperature and Rock Type

Additional Laboratory Activities

In addition to those activities motivated by the modeling programs, a number of studies were initiated to characterize the formation generally. X-ray diffraction traces of a large number of samples have been made; the results are summarized in Table 1. Analyses of the gases evolved upon

heating were made using a gas chromatograph-mass spectrometer. Water and carbon dioxide were evolved in appreciable quantities, but nothing was observed which would accentuate corrosion of equipment during the experiment. A number of shale samples were examined with a scanning electron microscope. In some samples, the shearing which was apparent in hand specimens could be seen to disrupt the fabric of the rock down to a scale of several microns. Heating of the samples did not appear to introduce obvious textural changes; however, it must be kept in mind that a SEM operates under a high vacuum, and any textural changes introduced merely by water loss would have occurred in both heated and unheated specimens. Pores in the rock did not seem to contain authigenic mineral growths. Due to the nature of the core material, it was not possible to obtain representative elastic and mechanical properties in the laboratory. Representative properties were therefore taken from the literature and used in subsequent modeling.

Modeling

Among available computer programs, two have been selected for modeling the observed temperature profiles. Initial concern was with the effects of heat conduction alone; consequently, pretest modeling was done using CINDA.² When it became apparent that boiling and condensation of water might influence the experiment, it was decided to try to model convection by using a code called SHAFT³ and by setting up bench-scaled experiments in a saturated medium of known porosity and permeability. Each of these efforts is briefly described below.

Most of the thermal modeling results reported here were generated using CINDA, a lumped parameter, and finite difference code. The node geometry presently used is illustrated in Fig. 30. Although the heat conduction is three-dimensional, it is treated here as axially symmetric. The program may be run using heater surface temperatures or input wattage as the controlled variable, either of which may be varied with time. As mentioned earlier, steam condenses in the space between the heater top and the packer. This was modeled by assuming a hole-wall temperature of 100°C

along this interval. The program may be used with either constant or temperature-dependent rock thermal conductivities. Output, as a function of time, is in the form of isotherms and either heater wattages or heater surface temperatures.

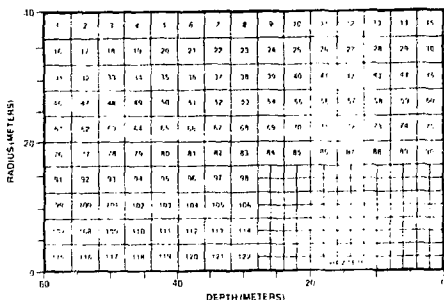


Fig. 30. Node Geometry Used in CINDA

SHAFT was used to investigate the nature of the convection cells initiated in the vicinity of the heater. A lumped parameter, finite difference numerical method is used to solve transient heat transfer and fluid flow equations in a porous medium. Fluid flow is based on Darcy flow; heat transfer is by conduction plus convection. The fluid may undergo a phase transformation; in this case, the transformation is the boiling of liquid water to make steam. To model a simple heat source implanted in a porous medium requires only a relatively simple node geometry (Fig. 31). With the presence of a cavity above the heater, however, the situation is far more complex and may exceed the state of the art in thermal modeling. Nevertheless, the attempt is made by assuming that the material in this region has a permeability of 100 darcies, as

compared to the value of 0.1 darcy selected for the rock. Consequently, steam formed in the heater hole may rise into the chimney with relative ease compared to its transfer into the adjacent rock. Because of the many small nodes in the heater area and the large changes in density and internal energy during boiling, the run time presently required for solution is longer than the actual time being modeled. The internal details of the code are being examined in an effort to remedy this situation.

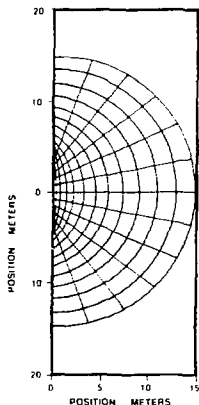


Fig. 31. Node Geometry Used in SHAFT³

A scaled laboratory experiment was carried out to gain some insight into the consequences of boiling at depth in a porous media. A 13 cm long by 1.3 cm diameter heater was emplaced one heater length below the "water table" in a plexiglass sandbox filled with water to a depth of 38 cm. Colored dyes were injected at various times to observe the pattern of convection. An array of thermocouples was situated in a plane parallel to, and about 0.64 cm back from, the front face. Temperatures were recorded as a function of time. Initially, the heater was held at just

below the boiling temperature for a week to establish steady state convection. The temperature was then slowly elevated to just above the boiling point, which represents more closely the actual situation that existed in the field. Shifts in the size or shape of the convection cells were noted and the wattage monitored to determine whether steam transport carried a significant fraction of the energy away from the heater. The size and shape of the vapor pocket was also noted. In addition to providing phenomenological information, the numerical data will serve to check predictions derived from SHAFT.

The mechanical response of the formation is being modeled using the SANDIA-BM1NES code.⁴ The following is a brief description of those aspects relevant specifically to the Conasauga project. A two-dimensional, axisymmetric study was made of the stress and deformation fields in the Conasauga shale heater experiment. The geometry being considered consists of a 40 meter (radius) by 60 meter (depth) region.

The heater is buried 15 meters deep at the center of the cylinder; it is assumed to have a length of 3 meters. By definition the hole has a diameter of 30 cm (1 ft). Details of heater construction were not modeled in this study since constraint conditions existing between the heater and the walls of the hole are not well defined. The mesh contains 235 bilinear, quadrilateral, isoparametric finite elements with 269 nodal points. The elements are concentrated in the region near the heater since the greatest stress and displacement gradients are anticipated in this area. Since the elastic properties of the Conasauga shale were not measurable, reasonable values were selected from the literature⁵ for use in this analysis:

- (1) $E = 10^{10}$ Pa, Young's Modules
- (2) $\nu = 0.3$, Poisson's Ratio
- (3) $\alpha = 10^{-5}/^{\circ}\text{C}$, Coefficient of Thermal Expansion

Future studies will assess the sensitivity of these results to the material properties selected.

Field Experimental Data

Thermal Analysis

Interpretation of the thermal data was directed toward obtaining in situ thermal properties of the formation, and toward gaining an idea of the dominant mechanisms of heat transfer in various regions around the heater. The approach was 1) model the site assuming conduction as the only form of heat transfer, and 2) by comparing calculated and actual isotherms, note where convection appeared to be important. Inferences based on this comparison were then compared to predictions from the two-phase fluid and heat transfer code, SHAFT. In this manner, it was possible to judge whether formation properties derived from a conduction-only model needed revision in light of the presence of ground water at the site.

Figure 32 is a schematic of the temperature fields parallel to strike at Sites One and Two 45 and 135 days after the heaters were activated. The upward opening of the isotherms reflects heat transfer outward through the walls of the open cavity between the top of the heater and the packer. Figures 33 and 34 are the radial temperature distributions parallel to strike at the heater midplane at 15-day intervals. It is of particular importance to note that after about thirty days the isotherms are no longer moving rapidly outward into the formation.

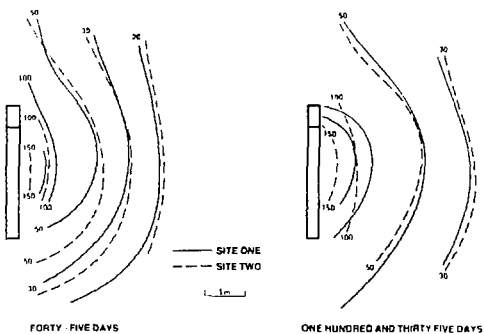


Fig. 32. Comparison Between Site One and Site Two Isotherms Parallel to Strike

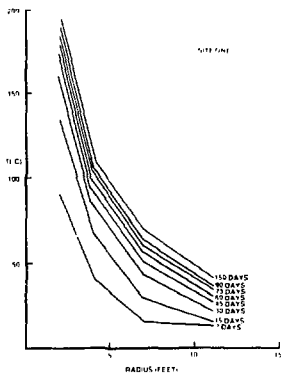


Fig. 33. Site One Radial Temperature Distribution

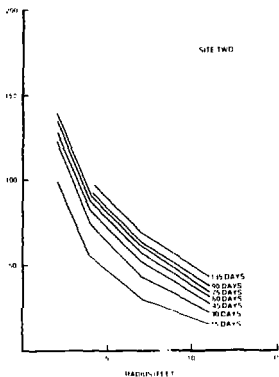


Fig. 34. Site Two Radial Temperature Distribution

As a prerequisite to further analysis it was necessary to verify that the isotherm positions in the field accurately reflected the total energy put into the formation over time. The first step in the analysis was to eliminate the possibility that through-flowing ground water had carried off a significant amount of the heater output. A comparison was made between the integrated heater wattage over time and the energy remaining in the formation. Table IV shows the comparison that was computed from isotherm positions and heat capacities (including a correction for boiling of three weight percent water). The data showed sufficiently close agreement that further analysis was undertaken. It should be noted that after about 100 days the low temperature isotherms had migrated beyond the last thermocouple arrays and therefore had precluded further energy balance estimates.

TABLE IV
Energy Input at Site One ($\times 10^{10}$ Joules)

<u>Time</u>	<u>Computed From Heater Power</u>	<u>Computed From Isotherms</u>
30 days	1.8	2.0
60 days	3.4	3.2
105 days	5.6	5.3

In order to generate a conduction solution for comparison with actual Conasauga isotherms, the computer code CINDA was used in conjunction with heater temperatures recorded during the test. It was also assumed that the heater hole was open for a distance of 3 meters above the heater and that the hole walls over this interval were to be maintained at 100°C. One final problem to be overcome was selection of a reasonable in situ thermal conductivity for use in the model. Solution was greatly facilitated by the observation that after thirty days, both output wattages of the heaters and isotherm positions had stabilized so that steady state heat conduction formulas could be applied to the field test data. Using temperature gradients in the formation at the heater midplanes and assuming the 50°C isotherm to be roughly spherical, it followed that thermal conductivities between 1.3 (Site One) and 1.8 (Site Two) W/m°C were required to dissipate the energy put into the formation by the heaters. In order to see whether in situ water loss had the same effect on thermal conductivity, as noted in the laboratory (Fig. 28), the region close to the heater at Site One was also examined. A steady-state line-source approximation over the temperature interval 100° to 200°C indicated that at Site One an effective conductivity of about 1.8 W/m°C was appropriate for this region. Apparently in situ conductivity of Conasauga shale does not decrease sharply when an area is dehydrated; an observation that is probably related to the confinement supplied by the surrounding formation and the weight of the overlying rock.

Because both the choice of isotherm location and temperature gradient are to a degree arbitrary, the in situ values were taken only as an indication of the range to be considered in formulating the model; a parametric study was carried out using temperature independent thermal conductivities of 1.5, 1.75, and 2.0 W/m°C. Assuming for the moment that convection plays a minor role in the heat transfer process, it follows from Fig. 35 that an in situ conductivity of about 2 W/m°C would be appropriate to account for the energy imparted to the formation. A comparison between actual and computed isotherms using this 2 W/m°C value is shown in Fig. 36. In the far field, agreement between computed and actual isotherms is good; but as one might expect, at temperatures above 100°C there is a consistent upward displacement of the field isotherms that may reflect the upward motion of steam. In this region, then, it was valid to inquire whether convection had seriously altered the heat flow pattern from what would be expected on the basis of conduction alone. The problem of modeling a heat source in a water-saturated porous medium was tractable using the code SHAFT if the cavity around the heater was omitted from the model. Figure 37 is a comparison of the predicted patterns of mass and heat flux assuming the formation to be isotropic and to have a permeability of 100 millidarcys. As one might anticipate, close to the heater the direction of fluid flow was found to be essentially vertical and of considerably greater magnitude than that observed in the far field environment. The energy flux, however, is roughly symmetrical around the heater midplane. This is expected when conduction is the only means of heat transport. Some perspective on the problem may be gained by noting that after sixty days, (the time for which Fig. 37 was computed), actual heater wattage at Site One was about 7 kW while the energy consumed to boil the water involved in the convection model was less than 1 kW. Even in the region close to the heater, conduction was the dominant mode of heat transfer; this strongly suggests that the initial estimates of in situ conductivity need not be revised to include the effects of convection at the site.

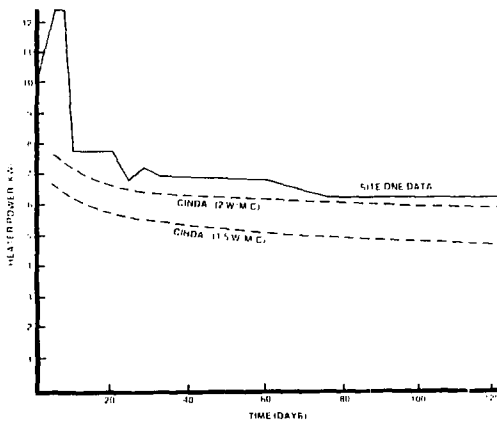


Fig. 35. Comparison Between Actual and Computed Power at Site One

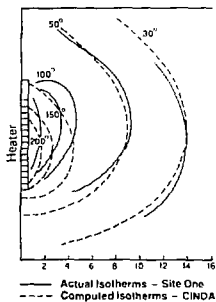


Fig. 36. Comparison Between Actual and Computed Isotherms at Site One ($^{\circ}\text{C}$)

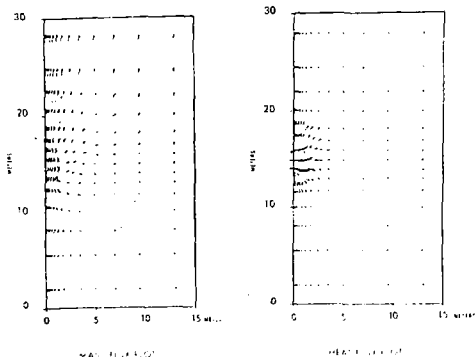


Fig. 37. Computed Circulation and Heat Flux

Mechanical Analysis

Figure 38 summarizes the extensometer data from Sites One and Two. Generally, motion is either undetectable, or points tend to move apart relative to one another. Relative movement was between 10^{-2} and 10^{-3} centimeter per centimeter of anchor separation.

Interpretation of these data was hindered by the limitations imposed by the extremely complex nature of the bedding planes and joint pattern present at the site. Nevertheless, it was possible to get reasonable agreement with the sense of expected motion, if not the magnitude, when a uniform positive thermal expansion was assumed along with an isotropic formation. In the V-shaped region extending horizontally from the heater midplane (see Fig. 39), extension is predicted, and was in fact observed. Above and below this region, compression is expected. However, due to the

paucity of instrumentation in this area, it is not possible to verify whether this motion occurred. Had the formation contracted, rather than expanded, the boundaries between the two regions would remain in the same position, but the sense of motion would have been reversed. A positive thermal expansion below 100°C is also consistent with the scant data available from the Creare gauges (Fig. 40) for that period of time when the gauge housings were not being affected by temperature changes. The discrepancy between the field data and the inferred behavior based on laboratory measurements again illustrates the important role played by the loss of water during laboratory measurements on argillaceous rocks. It is also apparent that only in the immediate vicinity of the heater will significant displacements occur, irrespective of whether expansion or contraction accompanies heating of the formation.

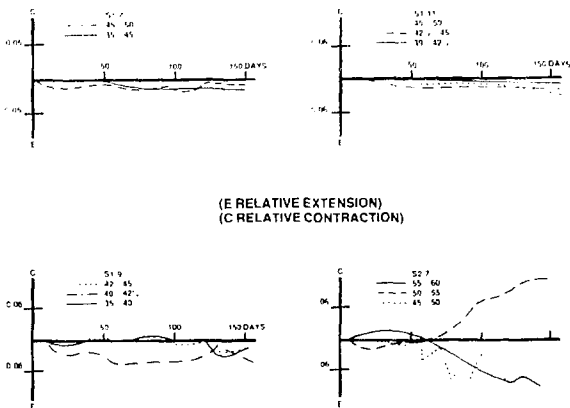
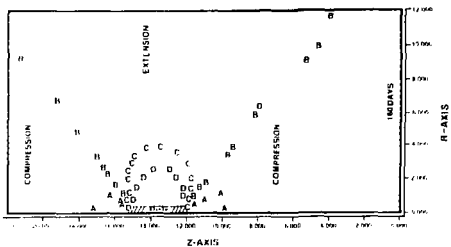


Fig. 38. Summary of Vertical Extensometer Data(hole numbers and extensometer anchor locations are indicated in the above key)



A, B, C, D - centimeters of motion per centimeter of initial and final separation

A denotes compression of 2×10^{-3} inches

B denotes 0 relative motion

C, D denote extension of 2×10^{-3} and 4×10^{-3} inches, respectively

Fig. 39. Predicted Regions of Vertical Extension and Compression (vertical and horizontal dimensions are in meters)

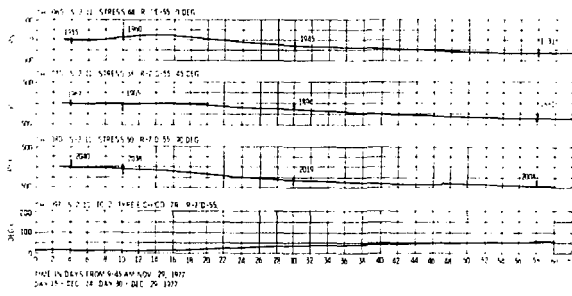


Fig. 40. Summary of Horizontal Creep Gauge Data. Zero degrees, 45 degrees, and 90 degrees denote the angle between the gauge axis and a radial vector from the heater hole passing through the gauge. The bottom trace shows the temperature at the gauge as a function of time. The useful portion of the stress (positive) is noted in the radial direction as is predicted by calculation assuming a positive thermal expansion coefficient.

VII. SUMMARY AND CONCLUSIONS

The Conasauga Experiments were not intended to fully answer the complex questions forwarded by the needs of nuclear waste disposal. Rather, the experiments were made to identify phenomena that may be of importance to the disposal problem, and may, indeed, indicate areas where future research would be most helpful. There is surprising good agreement between thermal models and field data. It was concluded, for instance, that many of the potentially troublesome features of the site proved little trouble. From the study, it seems safe to generalize, that, except where ground water circulation is demonstrably greater or the in situ contact resistance on cracks substantially higher, simple conduction models will suffice to give an accurate picture of the heat dissipation characteristics of the formation. It is less clear that such simplifying assumptions can be made in modeling a formation's mechanical response. Indeed, the textural variations from one locality to another in a "shale" are substantial; they are probably of sufficient importance to require additional testing before a general picture can emerge. It, therefore, seems appropriate to review some of our experiences as they pertain to the design of future experiments and, where possible, to recommend additional effort where it would be productive.

Site Selection

A number of major categories of argillaceous rocks may be defined on the basis of 1) texture (bedding, jointing, etc.), 2) mineralogy (illitic vs. montmorillonitic), and 3) other parameters such as organic and sulfide content, or hydrologic setting. In choosing a site for an experiment, careful consideration should be given whether those factors governing parameters of concern are, in fact, determinate in either a statistical or individual sense for the volume of rock to be affected by the test. Given the variability of argillaceous rocks, it is also evident that a variety of geologic settings require testing before generalization about the

behavior of a particular property can be made. Consideration should be given to the statistical significance of running two tests in even a relatively well-characterized geologic setting. In terms of simulating repository conditions, as opposed to code verification tests, it is obviously preferable to pick a site at depth, in a mine. For experiments not involving large quantities of radioactive materials, one might investigate the possibilities presented by coal, salt, or uranium mines in which shale is exposed. Even in the event of a near-surface experiment, siting in an abandoned quarry or strip mine is preferable to a setting where several meters of soil must be penetrated to reach bedrock. Regarding the specific problem presented by moderately jointed rocks, some understanding may be gained by choosing a region where joints are regularly spaced at intervals of one to several feet. One might then carry out scaled (bench) experiments on jointed blocks and use this response to model the expected displacement, thermal conductivity, etc., from a full-scale heater experiment. By characterizing individual jointed blocks, it should be possible to gain a statistical picture of the degree of variability in joint-surface characteristics over the site and from the field test assess whether this sort of joint seriously alters rock behavior. In the case of a pervasively jointed and bedded formation, it is evident that such an approach is not applicable; it may be that the only option available is that already carried out in the Conasauga Experiment. At the other extreme, the possibility of an unjointed shale has yet to be assessed experimentally. In this instance, it is probable that only a montmorillonitic shale will be found that has a suitable texture, and that water loss will play a significant role in its behavior.

Heater Design

Although the Conasauga heaters have performed satisfactorily, several modifications would be helpful. At present, it is thought necessary to cool the terminal region of these heaters by circulating air. It would be preferable to have a more corrosion-resistant terminal section and to eliminate the cooling air altogether. In any case, additional thermocouples should be installed along the various metal appendages

leading to the heater. There should be sufficient thermocouples to permit a rigorous calculation of the heat transfer along these members. Additional thermocouples on the heater surface would be helpful in delineating actual surface temperatures, a parameter of some considerable concern even in simple thermal analyses. Designing an internal heater element array would result in more uniform heater surface temperatures or perhaps in a distribution more representative of that expected on the external surface of an actual waste canister. In retrospect, the double redundancy of heating elements in the Conasauga heaters seems to be unnecessary. None of the heating elements have failed to date and even under the extremely wet conditions of the Conasauga Experiment the reserve heating capacity proved unnecessary. Finally, it is also necessary to have a good control on what the heater wattage is at all times, since energy balances are one of the more useful checks on formation behavior.

In the operation of the experiment, a number of problems arose due to the presence of a cavity above the heater. Initial attempts to decrease the size of this space by placing a packer at the base of the casing proved unsuccessful, and development of a reliable packer may be needed in future experimentation. An alternative possibility is that of back-filling the hole. The use of cement for this purpose clearly precludes heater recovery. However, if fine sand interspersed with thin layers of (less permeable) clay were used it might be possible to open the hole with a jet of compressed air (or water) in the event of an emergency or at the conclusion of the experiment. If during a future test an open cavity is to remain above a heater it should contain sufficient thermocouples to ensure that the temperature distribution throughout the cavity may be measured.

Site Instrumentation

Due to budget limitations, thermal instrumentation at the Conasauga Sites was not exhaustive. In retrospect, it is apparent, that some sensors should be emplaced along all four principal directions and preferably along some of the 45 degree directions as well. A complete

sensor array is particularly important in an anisotropic medium where convective fluid flow may be expected to play a part in heat transfer. In addition to thermocouples located at 0.61 m, 1.2 m, 2.1 m, and 3.3 m, it would also be highly desirable to have a means of sensing heater-hole wall temperatures and thermal couples at radii of 4.5, 6.0, and 7.6 meters. As far as depth of emplacement is concerned, coverage should extend from several meters below the bottom of the heater to a depth shallow enough so that it will be possible to close the isotherms in upward directions. It should be noted that drilling of the heater hole 0.6 meters from an open instrumentation hole did not result in breakthrough despite the friable nature of the Conasauga formation.

In situ determination of the mechanical response of a formation is most readily approached by measuring the actual displacements that occur in the field. A number of vertical extensometers were emplaced at various depths in the Conasauga tests; however, their number was wholly inadequate to characterize the response of a geologic setting as complex as that at the Conasauga site. On the basis of Fig. 40, 1) it is apparent that the positioning is most critical within a meter of the central heater site, and, 2) like the thermocouples, the array should extend over a considerable horizontal and vertical extent. In the Conasauga tests, the attempt was also made to measure the in situ stresses in three horizontal directions. Unfortunately, such measurements invariably depend on a displacement measurement and an equation relating this displacement to stress. In addition, problems were encountered in setting the gauges at the bottom of a drill hole. The number of stress gauges was also inadequate to characterize the behavior of that complex geologic setting. It follows, therefore, that in the immediate future, work should be directed towards developing reliable in situ displacement measurement techniques. If the operational problems could be overcome by choosing the site judiciously and by developing appropriate measurement techniques, it would be highly desirable to run a series of tests to determine whether existing computer codes are capable of predicting at least the displacement if not the stress, even in a very simple in situ geometry.

Instrumentation Development

Summaries of the inadequacies noted in the preceding pages or encountered during the fielding of the test are:

1. More reliable thermocouples are required for tests lasting in excess of several months. An alternate method of implanting thermocouples may be required. Several important thermocouples were lost during the test. It is possible that corrosion of the thermocouple sheaths was accentuated by the strongly basic environment. This corrosion apparently resulted from the sheaths being grouted in place. Alternatively, a temperature gradient of several hundred degrees over several meters may have resulted in one end becoming sufficiently anodic to accelerate corrosion of what is normally a relatively inert metal.

2. A reliable means of measuring heater-hole wall temperatures without disturbing heat transfer is desirable.

3. More developmental research is necessary before we can adequately measure a formation's mechanical response. First priority, however, should be given to developing a system capable of measuring lateral as well as vertical displacements in the walls of open holes because this problem is easier to solve than that of measuring stress. Next, the problem of stress determination should receive attention. It should be kept in mind that a) the system must operate in the field with its attendant wind and weather, b) measurements must be made at depths of many meters in holes but a few centimeters in diameter; c) some holes may have a pressure tight cap, d) the calibration must remain good over several hundred degrees centigrade and e) it must be possible to anchor the down-hole part of the sensor in rocks which may be of a highly friable nature.

4. An adaptation of the krypton-85 transmissivity apparatus to allow for periodic determinations during the course of a test without disturbing the conditions of the test would be most informative, particularly if it were developed in conjunction with an acoustic sensing system for

detecting cracking within the formation. This would help us determine when significant changes had occurred following a test of several months.

5. It would be helpful to develop a heat flux transducer capable of withstanding the rigors of a down hole environment and capable of functioning at several hundred degrees centigrade. Obviously, a means of implantation is also required.

Laboratory and Modeling Activities

In the field of rock mechanics, the mechanisms responsible for displacement and fracturing when the strain rates are very slow, require investigation and incorporation into predictive models. At present, the effects of in situ stresses, jointing, and bedding are also largely unexplored. In the field of material properties measurement, the importance of doing the tests in such a manner that the confining pressure and rate of dehydration match the field situation has been clearly illustrated. It is also evident that standard engineering measurements carried out on a small number of samples will not suffice to give a picture of a material's behavior that is adequate for the purposes of waste management. The effect of time has not been adequately studied. Chemical reactions involving silicates are typically sluggish; to accelerate the reactions by using elevated temperatures involves the risk that nonrepresentative mechanisms may dominate the behavior of the sample during the tests. At the earliest possible date, long-term laboratory tests at modest temperatures and pressures should be initiated. In light of our present lack of detailed knowledge, it is encouraging to remember that relatively simple models could be used to fit much of the Conasauge thermal data, and that the empirical parameters deduced from this fit were generally favorable for the purposes of waste disposal.

References

1. J. J. Dell'Amico, F. K. Captain, and S. H. Chansty, "Characterization and Thermal Conductivities of Some Samples of Conasauga Shale," ORNL-MIT-20, 1976.
2. Chrysler Improved Numerical Differencing Analyzer TN-AP-67-287, Chrysler Corporation Space Division, October 1967.
3. T. J. Lasseter, "Simultaneous Heat and Fluid Transport," ASME Paper 75-WA/HT-71, 1975.
4. J. R. Tillerson and M. M. Madsen, "Thermoelastic Capabilities for the Sandia-BMINES Program," SAND77-0378, Sandia Laboratories, NM, February 1978.
5. Technical Support for GEIS: Radioactive Waste Isolation in Geologic Formation, Vol. 6 Baseline Rock Properties - Shale, Y/OWL/TM-36/6 April 1978.

APPENDIX A

Grout Specifications

The grouts used for the Heater Experiments were designed to provide a material which is a reasonable match to the thermal conductivity properties of the rock in place. The cement content was reduced by the use of flyash (or Pozz) to keep the curing temperature of the grout below 150°F so that instrumentation cables would not be damaged. Two percent gel was added to reduce settling and bleeding before hardening. The standard grout was 50% cement/50% Pozz (by volume). For the holes containing stress gauges, expansive grouts were designed by substituting expansive cement for part (or all) of the Class A Portland Cement.

The weights of each material to provide 1 cubic meter of grout slurry are listed below (kg/m^3 of grout).

	<u>Standard 50/50 Pozz</u>	<u>Oak Ridge Expansive</u>
Class A Portland Cement	607	366
Chem Stress Cement	-	241
Chem Comp Cement	-	-
Flyash (Pozz)	472	472
Gel	21	21
Water	620	620

The physical properties for all grouts are as follows:

Density	1.69 g/cm ³
28-day Unconfined Compressive Strength	27.6 MPa
Coefficient of Thermal Expansion	11.2 °C ⁻¹
Thermal Conductivity, 16°C to 68°C	1.1 W/m°C